DOI:
10.1016/j.toxlet.2018.05.029

Document Version
Peer reviewed version

Title: Bringing *in vitro* analysis closer to *in vivo*: Studying doxorubicin toxicity and associated mechanisms in 3D human microtissues with PBPK-based dose modelling

Authors: Marcha Verheijen, Yannick Schrooders, Hans Gmuender, Ramona Nudischer, Olivia Clayton, James Hynes, Steven Niederer, Henrik Cordes, Lars Kuepfer, Jos Kleinjans, Florian Caiment

PII: S0378-4274(18)30226-1
DOI: https://doi.org/10.1016/j.toxlet.2018.05.029
Reference: TOXLET 10212

To appear in: *Toxicology Letters*

Received date: 16-1-2018
Revised date: 8-5-2018
Accepted date: 23-5-2018

Please cite this article as: Verheijen M, Schrooders Y, Gmuender H, Nudischer R, Clayton O, Hynes J, Niederer S, Cordes H, Kuepfer L, Kleinjans J, Caiment F, Bringing *in vitro* analysis closer to *in vivo*: Studying doxorubicin toxicity and associated mechanisms in 3D human microtissues with PBPK-based dose modelling, *Toxicology Letters* (2018), https://doi.org/10.1016/j.toxlet.2018.05.029

Bringing *in vitro* analysis closer to *in vivo*: Studying doxorubicin toxicity and associated mechanisms in 3D human microtissues with PBPK-based dose modelling

Marcha Verheijen[1], Yannick Schrooders[1], Hans Gmuender[2], Ramona Nudischer[3], Olivia Clayton[3], James Hynes[4], Steven Niederer[5], Henrik Cordes[6], Lars Kuepfer[6], Jos Kleinjans[1], Florian Caiment[1].

[1]Department of Toxicogenomics, Maastricht University, Maastricht, Netherlands

[2]Genedata AG, Basel, Switzerland

[3]Roche Pharmaceutical Research and Early Development, Roche Innovation Center Basel, Basel, Switzerland

[4]Luxcel Biosciences Ltd, Cork, Ireland

[5]Department of Imaging Sciences and BioMedical Engineering, King's College London, London, UK

[6]Institute of Applied Microbiology, RWTH, Aachen, Germany.

Corresponding author:

Marcha Verheijen
Department of Toxicogenomics, Maastricht University, P.O. Box 616, 6200 MD Maastricht, The Netherlands.
T: +31 43 3883986. F: +31 43 3884146. Email: marcha.verheijen@maastrichtuniversity.nl

Highlights

- We present an innovative *in vitro* model to better reflect the *in vivo* environment.
- Human 3D microtissues (co-culture of cardiomyocytes and fibroblasts) were used.
- Cells were exposed to PBPK-based repetitive dosing profile for two weeks.
- Our approach can retrieve mechanisms of DOX toxicity known to occur *in vivo*.
- Using physiologically relevant doses during toxicological research is important.

Abstract

Doxorubicin (DOX) is a chemotherapeutic agent of which the medical use is limited due to cardiotoxicity. While acute cardiotoxicity is reversible, chronic cardiotoxicity is persistent or progressive, dose-dependent and irreversible. While DOX mechanisms of action are not fully understood yet, 3 toxicity processes are known to occur *in vivo*: cardiomyocyte dysfunction, mitochondrial dysfunction and cell death. We present an *in vitro* experimental design aimed at detecting DOX-induced cardiotoxicity by obtaining a global view of the induced molecular mechanisms through RNA-sequencing. To better reflect the *in vivo* situation, human 3D cardiac microtissues were exposed to physiologically-based pharmacokinetic (PBPK) relevant doses of DOX for 2 weeks. We analysed a therapeutic and a toxic dosing profile. Transcriptomics analysis revealed significant gene expression changes in pathways related to "striated muscle contraction" and "respiratory electron transport", thus suggesting mitochondrial dysfunction as an underlying mechanism for cardiotoxicity. Furthermore, expression changes in mitochondrial processes differed significantly between the doses. Therapeutic dose reflects processes resembling the phenotype of delayed chronic cardiotoxicity, while toxic doses resembled acute cardiotoxicity. Overall, these results demonstrate the capability of our innovative *in vitro* approach to detect the three known mechanisms of DOX leading to toxicity, thus suggesting its potential relevance for reflecting the patient situation. Our study also demonstrated the importance of applying physiologically relevant doses during toxicological research, since mechanisms of acute and chronic toxicity differ.

Keywords

Doxorubicin, Cardiotoxicity, Transcriptomics, Physiologically-based pharmacokinetic modeling, 3D microtissues, mitochondrial dysfunction

1. Introduction

Doxorubicin (DOX, also known by the brand name Adriamycin) is a chemotherapeutic agent belonging to the class of anthracyclines, which are cytostatic antibiotics. DOX was isolated from *Streptomyces peucetius var. caesius* in 1967[1] and it is still one of the most frequently used anti-cancer agents for treating a variety of cancers (e.g. hematological cancers, soft-tissue tumors, and solid tumors), even though it causes severe side effects. Next to nausea, vomiting, alopecia, myelosuppression, stomatitis, and gastrointestinal disturbances, DOX is known to induce cardiotoxicity. Cardiotoxicity is classified as acute or chronic. Acute cardiotoxicity may already occur during treatment with a single high dose or within 2-3 days after multiple DOX treatments[2, 3]. Though its prevalence is higher than for chronic cardiotoxicity, these side effects are reversible and clinically manageable. A chronic cardiotoxic phenotype may emerge between one month and decades after DOX treatment. This persistent or progressive cardiotoxicity is dose-dependent and irreversible. In cases where congestive heart failure has developed, the prognosis for the patient is poor, with a mortality rate of 50% within one year[3-7]. Given this dose-dependency, a maximum cumulative dose of 450 – 600 mg/m^2 is recommended for DOX[8, 9].

DOX mechanisms of action are not fully understood yet. Nevertheless, it is generally accepted that the main mode of action is related to killing dividing cells. These effects are more severe for tumor cells since these cells divide more rapidly than non-cancer cells. However, DOX is not tumor cell-specific and can accumulate in the nucleus and mitochondria of heart, liver and blood cells, thereby contributing to toxic side effects, in particular chronic cardiotoxicity, even at therapeutic doses[5]. DOX has been found to 1) intercalate into DNA, 2) target DNA topoisomerases, and 3) generate reactive oxygen species (ROS) [10-12]. The first two processes inhibit unwinding of DNA, DNA replication, RNA transcription and protein biosynthesis. As a result, proliferation of dividing cells is also inhibited [9, 13]. This is thought to be the efficacy of the anti-cancer effects of DOX, while ROS generation is mainly ascribed to toxic effects[14]. ROS can be generated as a result of mitochondrial dysfunction, but also by the oxidative semiquinone formed at complex I of the electron transport chain (ETC) during DOX metabolism. The induced oxidative stress may damage cells and cause cell death[8, 11]. Other detrimental actions of DOX

can be related to death of non-cancer cells or to decreased cardiomyocyte functioning, which may partly result from mitochondrial dysfunction causing an imbalance in cellular energetics. Therefore, any effect of DOX on mitochondria structure or function can cause cardiomyocyte dysfunction and thereby cardiotoxicity[15]. The detrimental actions of DOX, known to occur *in vivo*, can thus be summarized into 3 toxicity processes: cardiomyocyte dysfunction, mitochondrial dysfunction and cell death. However, it should be noted that the split between efficacy and detrimental actions is not fully justified because of overlapping processes, such as oxidative stress and cell death.

To predict molecular mechanisms underlying long term toxicity, toxicological risk assessment traditionally relies on animal models[16]. However, notably due to increasing ethical pressure, the field has to reduce the amount of animal experiments. In this article, we present an innovative *in vitro* experimental design aimed to detect cardiotoxicity by obtaining a complete view of the induced mechanisms of a compound. By better reflecting the human *in vivo* conditions, we aim to find an *in vitro* model capable of reliably replacing animal models used within the field of toxicology and drug safety testing. First, instead of the regularly used monolayer cell cultures, a Human 3D cardiac microtissue (InSphero, SWL) model was used, which better resembles the *in vivo* heart [17-19]. This *in vitro* spheroid cell model contained approximately 4000 iPSC-derived human cardiomyocytes and 1000 cardiac fibroblasts. Second, in contrast to using a relatively high dose to treat the cells, physiologically based pharmacokinetic (PBPK) modelling[20] was included within the study design to better reflect the *in vivo* exposure. PBPK simulates the absorption, distribution, metabolism and excretion of a specific dose of DOX within the human body, therefore enabling us to predict the concentration to which a specific organ is exposed over time. The PBPK model was used to design a two weeks repetitive dosing profile in which microtissues were exposed to a decreasing dose over each day by means of 3 medium changes. The microtissues were exposed to either a therapeutic or a toxic dose of DOX using this PBPK-based repetitive dosing profile, and functional parameters for mitochondrial function and programmed cell death were assessed. Finally, by applying next-generation total RNA-sequencing to ribo-depleted RNA samples, we were able to analyze global changes in gene expression. By using this innovative experimental *in vitro* experimental design, we were able to successfully detect biological changes in the three main identified toxicity processes of DOX (cardiomyocyte dysfunction, mitochondrial dysfunction and cell death).

2. Methods

2.1 Samples

The human 3D cardiac microtissue (InSphero, SWL) model was used, containing approximately 4000 iPSC-derived human cardiomyocytes (female Caucasian donor) and 1000 cardiac fibroblasts (male Caucasian donor) per microtissue. The microtissues were cultured in 3D Insight™ Human Cardiac Microtissue Maintenance Medium (InSphero, Cat #CS-07-010-01).

2.2 PBPK model establishment

A PBPK model for DOX was established with the PBPK modelling software PK-Sim following a previously described workflow[21]. In particular, the model was used to quantify interstitial heart concentrations following administration of therapeutic and toxic drug doses. These concentration profiles were subsequently translated into discrete daily exposure profiles (Figure 1a, b). During model establishment, model predictions of blood plasma DOX concentrations were compared with literature data for parameter identification[22]. In a next step, the model was validated with further PK data4 (Figure 1c). Once daily therapeutic doses (0.415 mg*kg-1) were taken from literature while toxic doses (1.18 mg*kg-1) were estimated based on in vitro dose-response experiments. The toxic dose was estimated, such that the in vitro drug exposure (AUC) after 7 days resulting in a 20 % loss of cell viability (IC20) was equal to the unbound drug exposure in the interstitial heart compartment of the PBPK model after a 7 day once daily drug administration regimen (Figure 1a).

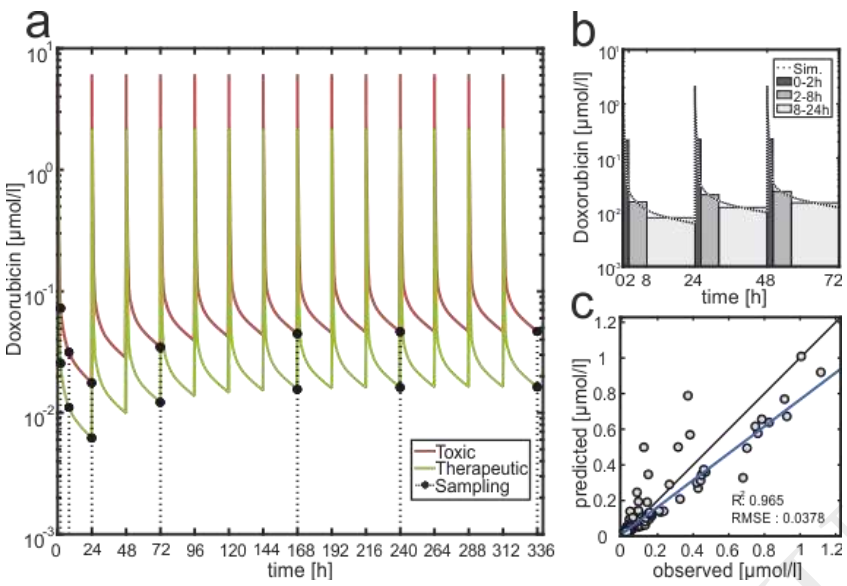

Figure 1: Doxorubicin PBPK model simulations. a) Simulations of DOX interstitial heart concentration profiles following a therapeutic (green) and toxic (red) once daily dosing regimen with experimental sampling points (black circles). b) Exemplary translation of PBPK simulations into discrete in vitro assay concentration with equal exposure, applied to cardiac microtissues for the first three days. c) Validation of PBPK model predicted DOX blood plasma concentrations with literature data[23].

2.3 Exposure

To accomplish the PBPK-based repetitive dosing profile described above, the medium of the microtissues was changed three times daily on working days with the PBPK-determined DOX concentrations (Sigma D1515, Cat #25316-40-9). These were administered using stock solutions of the compound dissolved in DMSO. As control, microtissues exposed to similar end concentrations of DMSO were used. 7 time points (2, 8, 24, 72, 168, 240 and 336 hours) were sampled in triplicate during the 2 weeks treatment period. For each sample, 36 microtissues were incubated separately, and subsequently pooled before RNA extraction in order to generate sufficient input material for NGS analysis.

2.4 RNA sequencing & Data processing

From the exposed microtissues, total RNA was isolated using Qiagen AllPrep DNA/RNA/miRNA Universal Kit (Cat #80224). The sample was depleted of ribosomal RNA using the Illumina RiboZero Gold kit (Cat #MRZG12324) and prepared for sequencing using Lexogen SENSE total RNA library preparation kit (Cat #009.96). After library preparation, the samples were sequenced on the HiSeq2500 (100bp paired-end). A pool of all DOX samples was sequenced on all 8 lanes of a flow cell. The same was done for the control samples. Control samples were sequenced with an average of 51.2 million raw reads, therapeutic DOX with 20.3 million reads and toxic DOX with 18.7 million. Because the sequencing reads still contained Lexogen adapter sequences, the first 12 bases of the 5'end of all reads were removed using

Trimmomatic version 0.32 [24]. The quality of the sequencing data was checked using FastQC version 0.11.3 [25] before and after trimming.

2.5 Gene expression analysis

For each sample, sequencing reads were mapped to the GENCODE version 26 (GRCh38) - Ensembl 88 (Comprehensive gene annotation) using the Genedata Profiler™ version 10.1, which incorporates the splice junction mapper STAR version 2.5.2b and Cufflinks based algorithms for transcript abundance estimation.

The quality of the samples was assessed according to the amount of (mapped) reads, Cook's distance, hierarchical clustering, principal component analysis, and sample dispersion. 1 replicate of DOX toxic 240h was excluded because of low read count.

Differentially expressed genes (DEGs) were determined using DESeq2 version 1.14.1 [26]. For each specific time point, 2 comparisons were performed: 1) therapeutic dose vs DMSO control; 2) toxic dose vs DMSO control. Samples of all time points for both doses were normalized together and the contrast function was used to extract differentially expressed genes for each time point, ensuring comparability between time points. Genes were being considered as differentially expressed when $q<0.05$.

2.6 Biological interpretation

For each dose and time point, lists of DEGs (depleted of ribosomal genes) were used as input for pathway over-representation analysis (ORA) using CPDB release 32 [27]. The Reactome database version 61 was selected because it is curated, focuses on molecular mechanisms and includes pathway hierarchy[28]. Results from this analysis was visualized using Omix visualization version 1.9.20 [29].

2.7 Functional assessments: ATP measurement, Caspase3/7 assay and Oxygen consumption

For measurement of ATP, Promega's CellTiter Glo 3D (Cat #G9683) was used according to manufacturer's protocol. In short, the microtissues were incubated for 30min with luciferase reagent and the luminescence was measured.

Apoptosis induction was measured using Promega's caspase-Glo® 3/7 assay (Cat #G8092) according to manufacturer's protocol. Briefly, the Z-DEVD-aminoluciferin substrate is cleaved by caspase 3/7, releasing a substrate for luciferase (aminoluciferin), resulting in measurable luminescence.

Mitochondrial function after 2 hours and 7 days of DOX treatment was assessed by measurement of extracellular oxygen consumption using Luxcel's MitoXpress® Xtra Oxygen Consumption Assay (Cat #MX-

200) according to manufacturer's protocol. In short, oxygen quenches the MitoXpress® Xtra probe, making the measured fluorescent signal, inversely proportional to the oxygen concentration.

2.8 Mitochondrial model

The computational mitochondrial model[30] for proteomics analysis was extended to evaluate the expression changes of genes functioning in mitochondria. The original model contained reactions of metabolites and involved protein complexes. For each protein complex represented in the model, the corresponding genes coding for each individual protein subunit were added.

3. Results

In order to investigate mechanisms of DOX-induced toxicity, human 3D cardiac microtissues were exposed to DOX for two weeks with either a therapeutic dose (D_{THE}) or a toxic dose (D_{TOX}) using a PBPK based dosing profile. To this end, the medium of the microtissues was changed three times per workday with a decreasing dose. Samples were generated after 2, 8, 72, 168, 240 and 336 hours of DOX exposure for both doses (Figure 2A).

Molecular effects of DOX on the cardiac cell were investigated using RNA-sequencing. The amount of differentially expressed genes (DEGs) increased over time (Figure 2B), except for a temporary decrease in DEGs at 240 hours of D_{THE}. Consistently across all time points, more DEGs were detected during exposure with D_{TOX} than with D_{THE}. Of these DEGs, 80% were protein-coding genes.

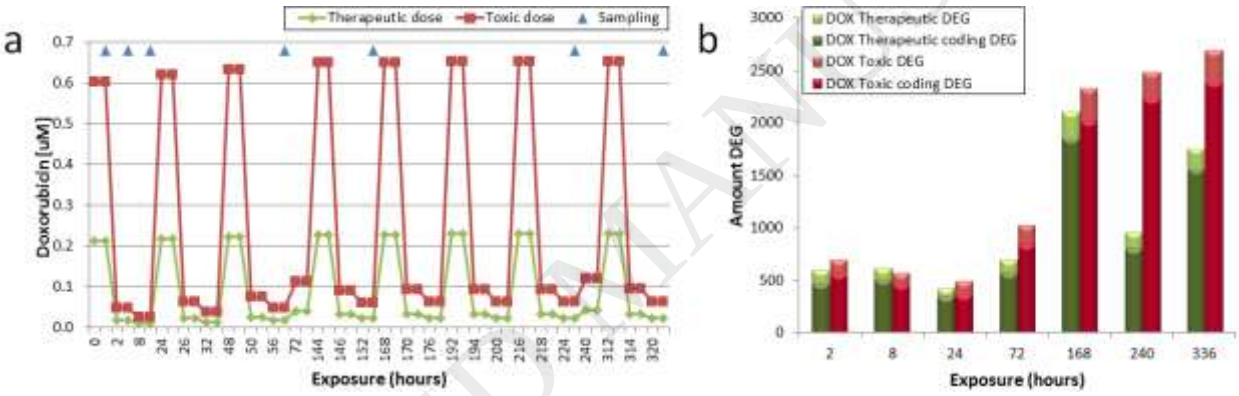

Figure 2: DOX exposure over time. A) PBPK-based dosing profile of cardiac microtissues, with D_{THE} in green and D_{TOX} in red. Times at which samples are obtained for analysis are depicted with blue triangles. B) Amount of DEGs detected at each time point, with D_{THE} in green, D_{TOX} in red and protein-coding DEGs in dark and non-coding DEGs in light.

3.1 Identifying known DOX pathways in vitro

An overview of the effects of DOX on the whole cardiac cell was investigated to identify processes linked to DOX toxicity. This was done through pathway overrepresentation analysis (ORA). Overrepresented pathways were visualized in supplementary figure 1. More significantly overrepresented pathways were identified for D_{THE} compared to D_{TOX}. This in combination with the higher amount of DEGs detected for D_{TOX} compared to D_{THE} indicates less specific cellular reactions for D_{TOX}. While therapeutic DOX exposure affects many cellular processes, the most significantly affected pathways throughout DOX treatment are "TCA cycle & respiratory electron transport" (q_{median} $2.92 \cdot 10^{-6}$) and "Striated muscle contraction" (q_{median} $9.3 \cdot 10^{-6}$). These pathways can be related back to detrimental actions of DOX. Therefore, toxicity processes (cardiomyocyte dysfunction, mitochondrial dysfunction and cell death) were investigated in

more detail (Figure 3), to determine whether our *in vitro* model expressed similar toxicity pathways as reported in literature for DOX.

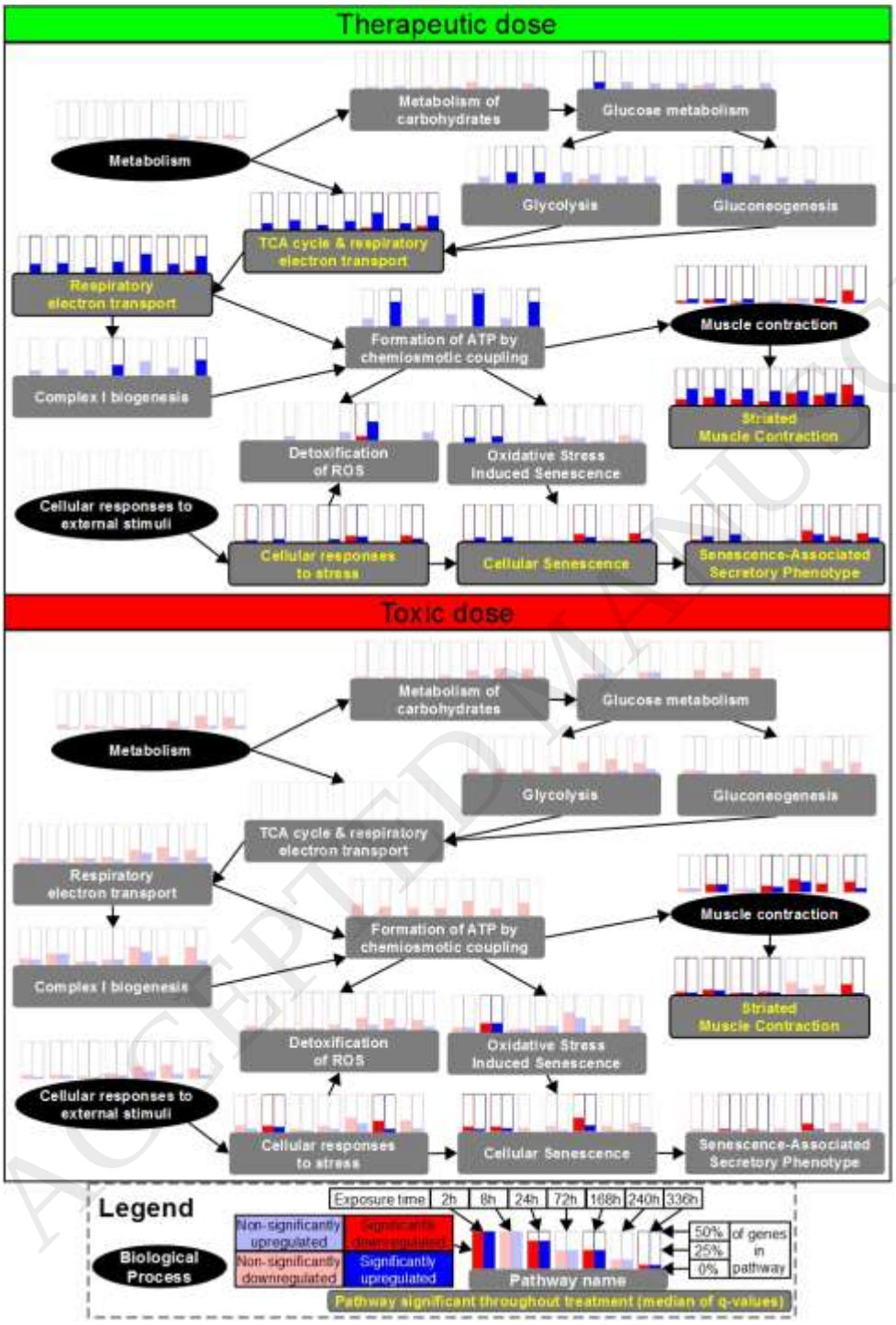

Figure 3: Specific toxicity processes affected by DOX. Visualization of overrepresented pathways, with D_{THE} on the left and D_{TOX} on the right. Black elipses identify clusters based on biological processes. Pathways (rectangles) were included when significantly overrepresented after DOX exposure minimally at 1 time point and at 1 dose, or in case the pathway was crucial for maintaining hierarchical links between the pathways. Coloured pathway names indicate pathways that were significantly overrepresented at the majority of time points (median of q-values <0.05). Bars on top of the pathway names depict up- and downregulation (blue and red resp.) per time point. The fill level corresponds to the percentage of DEGs detected (either up or down) in the pathway. The bars also depict if gene expression changes were significant at individual time points, with bright red and blue representing significant overrepresentation of the pathway at the specific time point, while faded colours are not significantly overrepresented at the given time.

Both DOX doses clearly induced “striated muscle contraction”, the main pathway related to cardiomyocyte dysfunction. Both doses displayed also a decreasing amount of upregulated genes over time combined with an increase of downregulated genes. For D_{TOX}, the amount of downregulated genes was always higher than of upregulated genes, while D_{THE} displayed more upregulated genes until 240 hour of treatment. In “cellular senescence”, more DEGs were observed for D_{TOX} compared to D_{THE}, while the pathway was found significantly overrepresented for D_{THE} at more time points than for D_{TOX}. This phenomenon is common in ORA and caused by the higher amount of DEGs and less specific cellular reactions of D_{TOX}. More striking were the differences between doses with respect to metabolic processes within the mitochondria. While D_{THE} induced upregulations over time, D_{TOX} induced downregulations at the end of the DOX treatment period(168h – 336h). Because mitochondria are involved in cell death and ATP generation necessary for cardiac contractile function, this dose-dependent difference in DOX-induced expressions of genes involved in mitochondrial processes may represent the underlying cause for differences in phenotypes for chronic or acute cardiotoxicity. Therefore, it is of interest to analyze mitochondrial dysfunction in more detail.

3.2 Functional assessment of microtissue viability

With respect to the ATP content of DOX-treated cells, the two analyzed doses (Figure 4A) were significantly different (p-value 0.027) from each other. For $D_{TOX,}$ ATP content decreases slightly until 72h, followed by a steep decrease in which ATP content is lower than the control. For $D_{THE,}$ a stable ATP content of approximately 20 pmol/microtissue is measured, except for a temporary drop at 240 hours of exposure. Between 24h and 168h, ATP content is increased compared to the DMSO controls. Relating these results to the gene expression changes observed in the pathway “Formation of ATP by chemiosmotic coupling”, indicates that increased gene expression is necessary for maintaining stable ATP content, while ATP content drops when no changes in gene expression are taking place. This suggests a decreased functionality and/or viability of the cardiac microtissues. Though cell death was not obviously detected on the gene level, this decreased viability was reflected from the caspase 3/7 assay results performed at 2 and 168 hours of DOX exposure (Figure 4b). Here, caspase activity was more than twice as high compared to UNTR (p_{2h}= 0.001; p_{168h}=0.022) ando D_{THE} (p_{2h}= 0.030; p_{168h}=0.039. This difference in cell viability was also indirectly confirmed by the size of the microtissues, which visually decreased over time for D_{TOX} but not for D_{THE}.

After 2 hours of DOX exposure, oxygen consumption was decreased by approximately 11% at both doses (p_{THE}= 0.061; p_{TOX}=0.048). After 168 hours of exposure, a difference oxygen consumption induced by the

two doses was visible, with a decrease of 15% (p=0.369) for D_{THE} and 33% for D_{TOX} (p=0.064). While the decrease for D_{TOX} can be partially caused by a lower amount of viable cells per microtissue, the decrease in oxygen consumption for D_{THE} suggests decreased mitochondrial function.

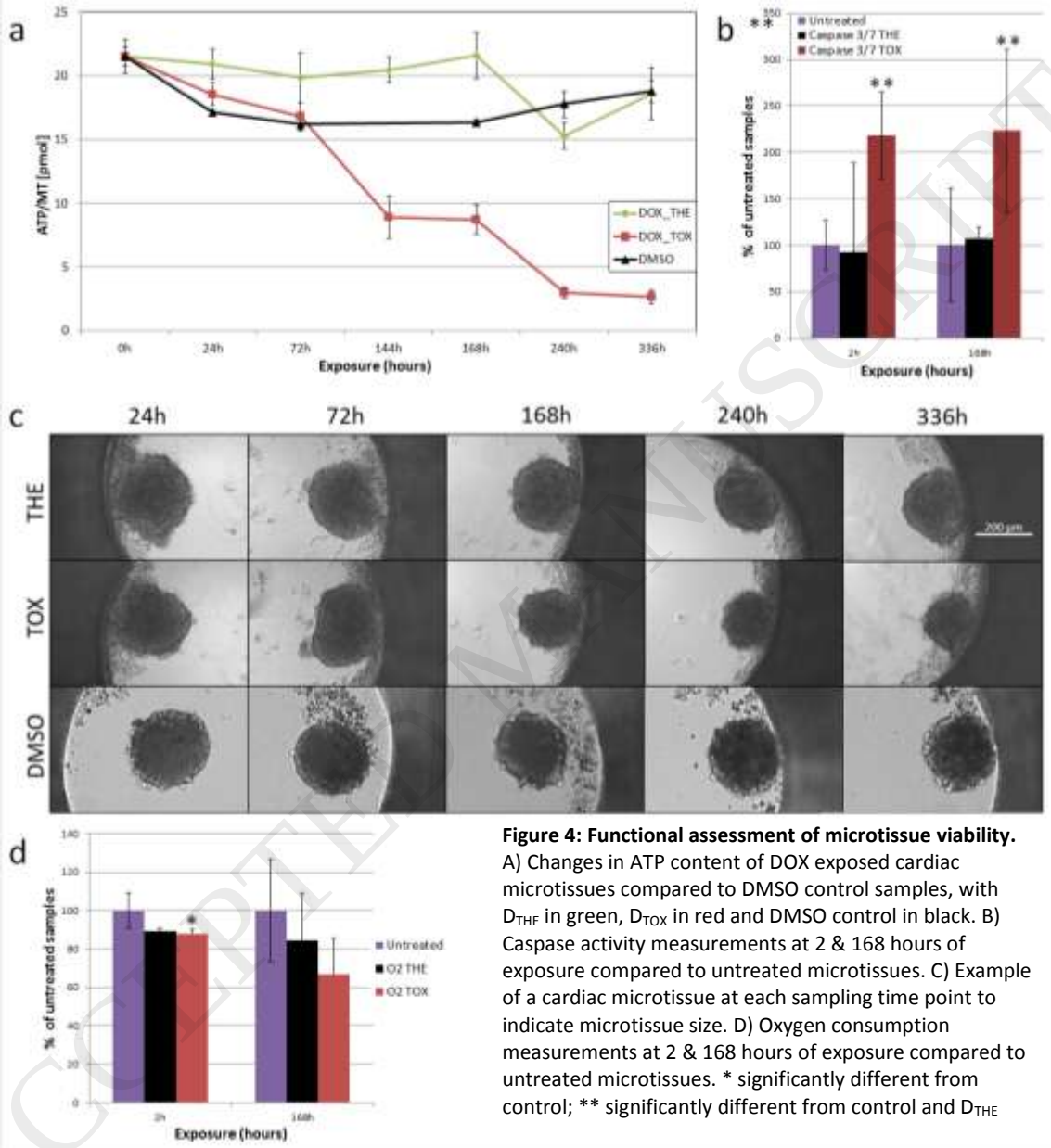

Figure 4: Functional assessment of microtissue viability. A) Changes in ATP content of DOX exposed cardiac microtissues compared to DMSO control samples, with D_{THE} in green, D_{TOX} in red and DMSO control in black. B) Caspase activity measurements at 2 & 168 hours of exposure compared to untreated microtissues. C) Example of a cardiac microtissue at each sampling time point to indicate microtissue size. D) Oxygen consumption measurements at 2 & 168 hours of exposure compared to untreated microtissues. * significantly different from control; ** significantly different from control and D_{THE}

3.3 Mitochondrial effects of DOX exposure

To elucidate the effects of DOX on genes functioning in mitochondria, DEGs were mapped onto the computational mitochondrial model [30] adapted for transcriptomics data (Figure 5). As expected, the mitochondrial model showed major differences between the two doses. D_{THE} displayed a majority of upregulated genes, while D_{TOX} displayed more downregulations, especially at later time points.

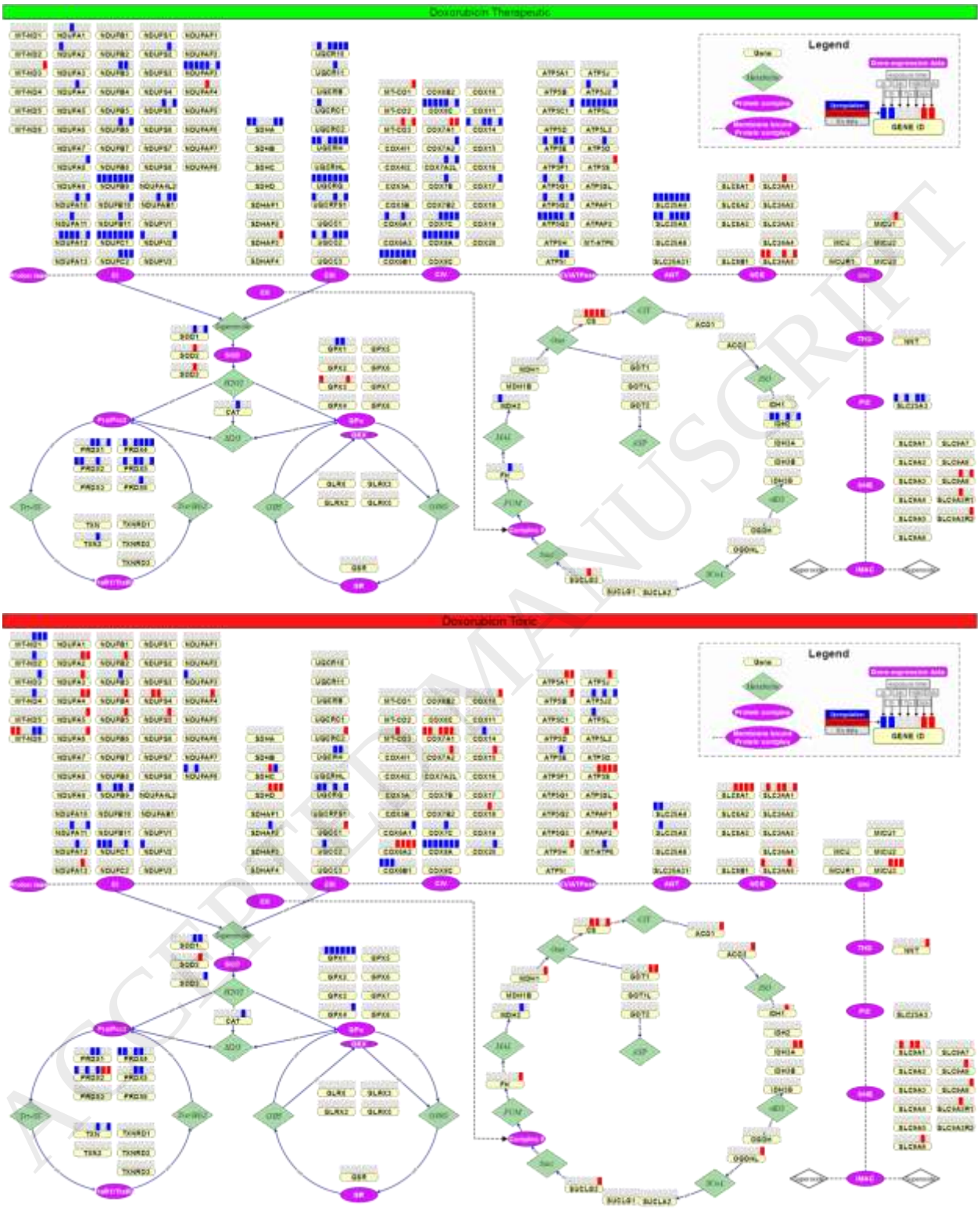

Figure 5: Transcriptomics mitochondria model showing effects of DOX on the mitochondria over time.
Upper panel display the therapeutic dose, lower panel correspond to the toxic dose. Purple ovals depict protein complexes and the genes encoding for subunits are displayed next to this in rectangles. On top of each gene, the boxes display the expression change over time, where each box corresponds to a specific time point (blue= upregulation, red= downregulation, grey= not significantly changed).

3.3.1 Detoxification of ROS

Detoxification of ROS (bottom left of Figure 5) was activated to the same extent for both doses, though there are slight differences in the final step of ROS detoxification, in which H_2O_2 is converted to water. While for D_{THE} this reaction was mainly catalyzed by peroxiredoxin (*PRX*), for D_{TOX} this reaction was carried out by both peroxiredoxin (*PRX*) and glutathione peroxidase (*GPx*). Overall, the upregulations found in these ROS detoxification genes indirectly indicated an increase in ROS formation in response to DOX.

3.3.2 Electron transport chain and formation of ATP

Table 1: DOX effect on ETC complexes, overview of affected genes at minimally one time point

Complex	Genes in complex	Affected genes (number / % of complex)		Genes upregulated (number / % of complex)		Genes downregulated (number / % of complex)		Genes significant >4 time points (number / % of complex)	
		D_{THE}	D_{TOX}	D_{THE}	D_{THE}	D_{TOX}	D_{TOX}	D_{THE}	D_{TOX}
I	53	21 / 39.6	25 / 47.2	19 / 35.8	2 / 3.8	12 / 22.6	12 / 22.6	NDUFA12, NDUFB9, NDUFC1, NDUFAF3	MT-ND6, NDUFB9, NDUFC1
II	8	2 / 25.0	3 / 37.5	1 / 12.5	1 / 12.5	1 / 12.5	1 / 12.5	SDHA	-
III	12	7 / 58.3	5 / 41.7	7 / 58.3	0	2 / 16.7	3 / 25.0	UQCR10, UQCRH, UQCRQ, UQCC2	UQCRQ
IV	29	13 / 44.8	13 / 44.8	10 / 34.5	3 / 10.3	7 / 24.1	6 / 20.7	COX6B1, COX6C, COX7C, COX8A, COX14	COX6A2, COX7A1, COX8A
V	21	11 / 52.4	12 / 57.1	10 / 47.6	1 / 4.8	8 / 38.1	4 / 19.0	ATP5E, ATPG3, ATP5L	ATP5S

Dose-dependent differences were most noticeable in the complexes of the ETC (top left of Figure 5). The overall amount of genes affected (minimally at 1 time point) was similar between the doses, with complex I expressing the most DEGs. Because of the difference in amount of genes per complex, comparison in percentage of complex gave a better overview of the DOX effect (Table 1). Complex III was mostly affected for D_{THE}, while complex V (also known as ATP synthase) was highly affected by both doses. Complex II was the least affected by DOX exposure. Dose-dependent differences were mostly observed through the direction of expression changes. Affected genes for D_{THE} were mostly upregulated, while D_{TOX} displayed an increase in downregulated genes, especially in later time points. Names of genes that were most highly affected by DOX exposure (significantly affected minimally at 4 time points) were also included in Table 1. Figure 6 depicts the log2 fold changes of these genes. Only gene expression changes of highly affected complex V genes were highly correlated to the changes observed in ATP

content (Figure 4A), suggesting that the ATP level modification induced by DOX are directly monitored by the expression level of the genes involved in complex V.

Overall, DOX-induced gene expression changes in the ETC were observed at both doses, though these changes indicate different underlying processes between the doses, discriminating between the phenotype of delayed chronic cardiac toxicity and acute cardiotoxicity.

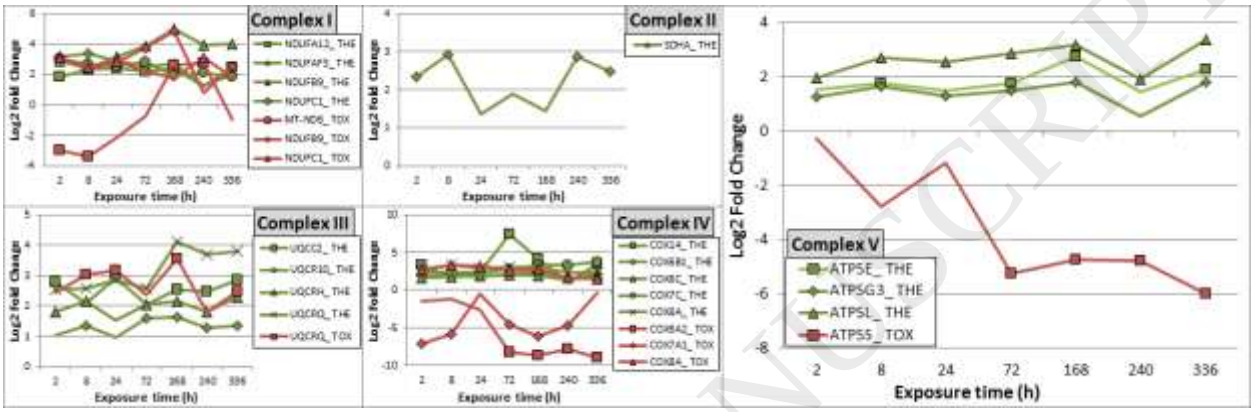

Figure 6: Log2 fold changes of highly affected ETC genes. Genes with significant expression changes minimally at 4 time points were depicted for each ETC complex, with D_{THE} in green and D_{TOX} in red. Significant log2 fold changes are indicated with a marker, while non-significant changes are depicted with only a line.

4. Discussion

The main objective of this study was to validate our novel *in vitro* experimental design for its use in predictive toxicological research. For this purpose, we analyzed cardiotoxic effects of doxorubicin (DOX). Our *in vitro* approach was designed to improve the resemblance to *in vivo* situations. This was achieved by using novel human 3D cardiac microtissues. This spheroid cell model contains a co-culture of iPSC-derived human cardiomyocytes and cardiac fibroblasts, better resembling the *in vivo* heart than mono-culture monolayers. Furthermore, while standard toxicological research is being done with short time series and exposures at one specific dose, we applied a 2 week PBPK-based repetitive dosing profile that resembles *in vivo* drug concentrations in patients with one drug administration per day. The dose of DOX to which a patient's heart is exposed was calculated based on pharmacokinetic simulations of the absorption, distribution, metabolism and excretion of DOX. *In vitro*, the medium of the cardiac microtissues was changed three times daily with calculated DOX doses, resulting in the highest dose in the morning and the lowest dose in the evening of each working day during the 2 week exposure. The experimental design also included the exposure of two different dosing profiles, one based on therapeutic doses, as administered to a patient, and one based on a toxic dose. From these samples,

RNA was extracted and sequenced to determine if this novel *in vitro* approach is able to retrieve the *in vivo* toxicity mechanisms known for DOX.

We used three detrimental actions of DOX which are known to occur *in vivo* (cardiomyocyte dysfunction, mitochondrial dysfunction and cell death) to determine that the *in vitro* approach was able to retrieve the *in vivo* toxicity pathways known for DOX [8, 11, 14, 15]. Results from ORA indicated less specific cellular reactions for D_{TOX}, observed by the combination of more DEGs and less overrepresented pathways compared to D_{THE}. Furthermore, ORA identified toxicity of DOX by gene expression changes in the pathways of "striated muscle contraction", "TCA cycle & respiratory electron transport" and "cellular senescence". Gene expression changes in "striated muscle contraction" (cardiac function) and "cellular senescence" (cell death) displayed similar patterns, while mitochondrial processes ("TCA cycle & respiratory electron transport") displayed significantly upregulated processes for D_{THE} and non-significantly downregulated processes for D_{TOX}. A central link between the toxicity pathways is the "formation of ATP by chemiosmotic coupling". Mitochondrial gene expression changes correlated with ATP measurements, in which D_{THE} displays a relatively stable ATP content, while ATP content for D_{TOX} decreased drastically over time. From this, we hypothesize that both doses induce toxicity, but the underlying processes between the doses are different, with its origin resulting from differences in mitochondrial functioning. Therapeutic doses reflect processes underlying the phenotype of delayed chronic cardiac toxicity, while toxic doses reflect processes of acute cardiotoxicity.

A more detailed analysis of mitochondrial dysfunction was done by investigating the 5 complexes of the ETC and activation of ROS detoxification processes. Mainly complex I, but also complex III, represent the sites of premature electron leakage to oxygen, resulting in the generation of ROS. Inefficiency of complex I can therefore result in increased ROS generation and oxidative stress. Furthermore, complex I is also a known interaction site for DOX, where it is reduced to form the oxidative semiquinone, which in turn, reduces oxygen to the highly reactive superoxide, returning DOX to its original state. Besides functioning as signaling molecules, ROS can damage proteins, nucleic acids and lipids in the cell. In order to prevent this, the cell is equipped with mechanisms to detoxify ROS. Gene expression changes indicated a similar increase in ROS detoxification between the doses. This confirms that ROS generation induced by DOX is indeed taking place in the *in vitro* model. Generated ROS is part of a positive feedback loop, in which more ROS results in more mitochondrial DNA (mtDNA) damage, leading to defects in the ETC complex, which results in increased ROS formation. Though uncertain whether this loop is initiated

by generated ROS or if mtDNA damage is induced by DOX directly, this could explain the persistent and cumulative nature of DOX cardiotoxicity, even in the absence of the drug itself [5].

The detailed mitochondrial model also revealed major effects of DOX on the ETC and ATP production. Changes in this process differed significantly between the doses, with upregulations across time for D_{THE} and a majority of downregulations in later times for D_{TOX}. Most DEGs were detected in Complex I for both doses. Complex I is the starting point for transferring electrons form NADH through the ETC in order to generate ATP [31, 32]. Also highly affected was Complex V (ATP synthase), which acts as a membrane channel for protons to be returned to the matrix. The flow back of protons gains the energy needed to convert ADP to ATP. The intermediate complexes of the ETC were also affected, though complex II only slightly. Because complex II is the only ETC complex that is completely encoded by the nucleus, and therefore less susceptible to mitochondrial ROS[14], this strengthens the involvement of the previously noted positive feedback loop between ROS, mtDNA damage and defects in ETC complexes. This process is also supported by the expression profile in mitochondrial encoded genes for subunits of complex I (MT-ND genes), which displayed changes in toxic dose, but not in therapeutic dose.

The downregulations in gene expression at the later time points of toxic DOX exposure indicates the failure of ATP production through ETC. The decrease in ATP content of the microtissues was a continuous process throughout the exposure, a pattern that was also observed for ATP5S, the most affected gene in complex V. This gene, also known as factor B, is responsible for the energy transduction activity of the ATP synthase complex[33]. Though, it is unlikely that a defect of this one gene was solely responsible for the ATP decrease. Decreased effectiveness of the ETC may also be due to decreased oxygen availability, oxygen being consumed by DOX during ROS generation. Therefore, the ETC has less protons available to establish the proton gradient necessary for ATP production [14]. However, it seems more likely that the heterogeneity of DOX exposure causes malfunctioning cells in the outer layers of the microtissue to die, leaving a decreased amount of viable cells at the core to produce ATP. Because RNA-sequencing detects the mean gene expression of all living cells in the sample, this effect might not be significantly present to be detected in our data analysis. The detected decrease in gene expression at later time points therefore indicates adversity of the microtissue. This adversity was also observed in pathway analysis, where cellular processes are affected in less specific ways, indicating deregulation of the cell which may result in cell death. Though not observed by gene expression changes, cell death is observed in the cardiac microtissues at toxic doses of DOX through a decrease in microtissue size and increase of caspase 3/7 activity.

In microtissues exposed to therapeutic doses, the DOX effect was also not equally distributed over the mitochondria present in the cells of the cardiac microtissue. Only a small amount of cells in the outer layer of the microtissue died, as could be seen from the small increase in caspase activity and a decrease in microtissue size that is hardly visible. However, an increase in gene expression of mitochondrial and ETC genes was necessary in order to maintain cellular ATP content, indicating a possible adaptation response in which less affected mitochondria compensate for highly affected mitochondria. However, this adaptation response may not be sufficient for maintaining cardiac function, because genes involved in striated muscle contraction were already showing decreasing expression level. Since the regenerative capacity of the heart is limited to ventricular remodelling, cumulative toxicity surpasses the point to which the organ can adapt, thereafter resulting in a delayed phenotype of heart failure, as is observed in patients with chronic cardiotoxicity after DOX treatment [4, 15].

5. Conclusion

Overall, these results confirm that our *in vitro* approach, based on 3D human microtissues exposed to an innovative 2 weeks PBPK dosing profile of DOX, is able to retrieve the known mechanisms of DOX toxicity. This new *in vitro* toxicity model can be extended to other 3D human microtissues, such as the already available liver model from primary hepatocytes.

The insights from the current study demonstrate the importance of applying physiologically relevant dosing profiles during toxicological research. Many studies on DOX effects have been performed with single and/or extremely high doses that do not reflect - and may even obscure - the true mechanisms of toxicity. Therefore, controversy in published results must be treated cautiously because of the risk of oversimplification and mixture of the different mechanisms of acute and chronic effects [14, 34]. Ultimately, we believe that this novel approach, better mimicking the human *in vivo* condition, could replace animal models within the field of toxicology and drug safety testing.

Conflict of Interest

The authors declare that there are no conflicts of interest.

Acknowledgements

This work was supported by the HeCaToS project as part of the EU Seventh Framework Programme (602156).

References

1. Arcamone, F., et al., *Patent application Farmitalia Research Laboratories.* NSA, 1967. **251**.
2. Zhang, Y.W., et al., *Cardiomyocyte death in doxorubicin-induced cardiotoxicity.* Archivum Immunologiae Et Therapiae Experimentalis, 2009. **57**(6): p. 435-445.
3. Chatterjee, K., et al., *Doxorubicin Cardiomyopathy.* Cardiology, 2010. **115**(2): p. 155-162.
4. Chen, B., et al., *Molecular and cellular mechanisms of anthracycline cardiotoxicity.* Cardiovascular Toxicology, 2007. **7**(2): p. 114-121.
5. Carvalho, F.S., et al., *Doxorubicin-Induced Cardiotoxicity: From Bioenergetic Failure and Cell Death to Cardiomyopathy.* Medicinal Research Reviews, 2014. **34**(1): p. 106-135.
6. Kumar, S., et al., *Doxorubicin-induced cardiomyopathy 17 years after chemotherapy.* Tex Heart Inst J, 2012. **39**(3): p. 424-7.
7. Takemura, G. and H. Fujiwara, *Doxorubicin-induced cardiomyopathy from the cardiotoxic mechanisms to management.* Prog Cardiovasc Dis, 2007. **49**(5): p. 330-52.
8. Varga, Z.V., et al., *Drug-induced mitochondrial dysfunction and cardiotoxicity.* Am J Physiol Heart Circ Physiol, 2015. **309**(9): p. H1453-67.
9. Edwardson, D.W., et al., *Role of Drug Metabolism in the Cytotoxicity and Clinical Efficacy of Anthracyclines.* Curr Drug Metab, 2015. **16**(6): p. 412-26.
10. Damiani, R.M., et al., *Pathways of cardiac toxicity: comparison between chemotherapeutic drugs doxorubicin and mitoxantrone.* Archives of Toxicology, 2016. **90**(9): p. 2063-2076.
11. Sorensen, J.C., et al., *Mitochondria: Inadvertent targets in chemotherapy-induced skeletal muscle toxicity and wasting?* Cancer Chemother Pharmacol, 2016. **78**(4): p. 673-83.
12. Burridge, P.W., et al., *Human induced pluripotent stem cell-derived cardiomyocytes recapitulate the predilection of breast cancer patients to doxorubicin-induced cardiotoxicity.* Nat Med, 2016. **22**(5): p. 547-56.
13. Yang, F., et al., *Doxorubicin, DNA torsion, and chromatin dynamics.* Biochim Biophys Acta, 2014. **1845**(1): p. 84-9.
14. Berthiaume, J.M. and K.B. Wallace, *Adriamycin-induced oxidative mitochondrial cardiotoxicity.* Cell Biology and Toxicology, 2007. **23**(1): p. 15-25.
15. Tokarska-Schlattner, M., et al., *New insights into doxorubicin-induced cardiotoxicity: The critical role of cellular energetics.* Journal of Molecular and Cellular Cardiology, 2006. **41**(3): p. 389-405.
16. Verheijen, M., et al., *Development and regulatory application of microRNA biomarkers.* Biomarkers in Medicine, 2015. **9**(11): p. 1137-1151.
17. Elliott, N.T. and F. Yuan, *A review of three-dimensional in vitro tissue models for drug discovery and transport studies.* J Pharm Sci, 2011. **100**(1): p. 59-74.
18. Achilli, T.M., J. Meyer, and J.R. Morgan, *Advances in the formation, use and understanding of multi-cellular spheroids.* Expert Opinion on Biological Therapy, 2012. **12**(10): p. 1347-1360.
19. Zuppinger, C., *3D culture for cardiac cells.* Biochimica Et Biophysica Acta-Molecular Cell Research, 2016. **1863**(7): p. 1873-1881.
20. Kuepfer, L., et al., *A model-based assay design to reproduce in vivo patterns of acute drug-induced toxicity.* Archives of Toxicology, 2017: p. 1-3.
21. Kuepfer, L., et al., *PBPK Modelling of Intracellular Drug Delivery Through Active and Passive Transport Processes*, in *Intracellular Delivery III: Market Entry Barriers of Nanomedicines*, A. Prokop and V. Weissig, Editors. 2016, Springer International Publishing: Cham. p. 363-374.
22. Speth, P.A., et al., *Cellular and plasma adriamycin concentrations in long-term infusion therapy of leukemia patients.* Cancer Chemother Pharmacol, 1987. **20**(4): p. 305-10.
23. Eksborg, S., et al., *Pharmacokinetic study of IV infusions of adriamycin.* European Journal of Clinical Pharmacology, 1985. **28**(2): p. 205-212.

24. Bolger, A.M., M. Lohse, and B. Usadel, *Trimmomatic: a flexible trimmer for Illumina sequence data.* Bioinformatics, 2014. **30**(15): p. 2114-2120.
25. Andrews, S., *FastQC: a quality control tool for high throughput sequence data.* http://www.bioinformatics.babraham.ac.uk/projects/fastqc, 2010.
26. Love, M.I., W. Huber, and S. Anders, *Moderated estimation of fold change and dispersion for RNA-seq data with DESeq2.* Genome Biology, 2014. **15**(12).
27. Kamburov, A., et al., *ConsensusPathDB: toward a more complete picture of cell biology.* Nucleic Acids Research, 2011. **39**: p. D712-D717.
28. Fabregat, A., et al., *The Reactome pathway Knowledgebase.* Nucleic Acids Research, 2016. **44**(D1): p. D481-D487.
29. Droste, P., et al., *Visualizing multi-omics data in metabolic networks with the software Omix: a case study.* Biosystems, 2011. **105**(2): p. 154-61.
30. de Oliveira, B. and S. Niederer, *Computational models of doxorubicin mitochondria cardiotoxicity.* Journal of Pharmacological and Toxicological Methods, 2016. **81**: p. 349-349.
31. Cooper, G.M. and R.E. Hausman, *The cell : a molecular approach*. Sixth edition. ed. 2013, Sunderland, Massachusetts: Sinauer Associates. xxiii, 832 pages.
32. Alberts, B., et al., *Molecular biology of the cell*. Sixth edition ed. 2014, New York: Garland Science. xxxiv, 1342, 34, 53, 1 pages.
33. Belogrudov, G.I. and Y. Hatefi, *Factor B and the mitochondrial ATP synthase complex.* J Biol Chem, 2002. **277**(8): p. 6097-103.
34. Simunek, T., et al., *Anthracycline-induced cardiotoxicity: Overview of studies examining the roles of oxidative stress and free cellular iron.* Pharmacological Reports, 2009. **61**(1): p. 154-171.